

# TESTING OF THE TORSIONAL STIFFNESS OF THE PASSENGER CAR FRAME AND ITS VALIDATION BY MEANS OF FINITE ELEMENT ANALYSIS

KRZYSZTOF PODKOWSKI<sup>1</sup>, ADRIAN MALCZUK<sup>2</sup>, ANDRZEJ STASIAK<sup>3</sup>, MACIEJ PAWLAK<sup>4</sup>

## Abstract

The paper presents the results of the conducted tests of torsional stiffness of the VOSCO S106 passenger car, as well as the validation process of these tests by means of numerical analyses using the FEM finite element method. The most important element of the vehicle structure is the part of the spatial frame or the safety cage. Engine, brake system, fuel system and steering system, suspension as well as body and parts, their mounting nodes, hinges, locks, etc. are attached to the frame. The frame must therefore have adequate strength to protect the driver in the event of a tipover or impact. The frame is usually made of steel pipes with the prescribed dimensions and strength according to regulations. The torsional stiffness of the vehicle chassis has a significant influence on its driveability and therefore is an important parameter to measure. In this article, the torsional stiffness of the vehicle frame is calculated experimentally, which was then verified by finite element analysis (FEM) using the Altair HyperWorks program.

**Keywords:** vehicle torsional stiffness; FEM; FEA; validation; passive safety of the vehicle

## 1. Introduction

To check the torsional stiffness of the frame experimentally, a special support structure has been made, and fastening brackets have been made to reduce displacement and rotation from all axes and directions [41]. A load was also applied and the deflection was measured using a dial indicator.

A similar design has been modelled in the HyperMesh program [27]. A surface mesh was created and a load was defined which was equivalent to the mass used to twist the frame in the test on the real object. The measured deflection was compared with the experimental value for its validation.

1 Department of Engineering and Numerical Analysis, R&D Network Łukasiewicz - Automotive Industry Institute, 55 Jagiellonska str., 03-301 Warsaw, Polska, e-mail: k.podkowski@pimot.eu

2 Department of Engineering and Numerical Analysis, R&D Network Łukasiewicz - Automotive Industry Institute, 55 Jagiellonska str., 03-301 Warsaw, Polska

3 Chief Designer/Design Department, Fabryka Samochodów Osobowych Syrena W Kutnie S.A., Józefów 9, 99-300 Kutno, Polska

4 Plant Manager/Management Board, Fabryka Samochodów Osobowych Syrena W Kutnie S.A., Józefów 9, 99-300 Kutno, Polska

The torsional stiffness of the vehicle chassis has a significant influence on its driveability and therefore is an important parameter to measure [3, 5, 8]. The greatest effect of torsional deformation can be found with transverse load transfer between the front and rear axes [4, 7]. During steady-state rotation, the infinitely rigid frame will cause both the front and rear tilting angle to be the same, as it is assumed during the calculation of the suspension structure [28, 32]. Permission to turn in the chassis will redistribute some mass transfer between the front and rear tires, making these values deviate from their designed values. For most racing vehicles, the frame is stiffer than the suspension stiffness is designed [1, 29, 38]. Based on the provided materials in the form of 3D CAD models and additional information such as: the names of the materials envisaged, the expected ways of joining elements, a discreet model of the vehicle frame was prepared. The carried out work included:

- analysis of the 3D CAD model of the vehicle frame structure;
- development of calculation models based on the obtained 3D model;
- determination of load patterns, mounting and other boundary conditions;
- development of a grid in the Altair HyperMesh program;
- defining welded and bolted joints using dedicated functional components of the numeric solver;
- numerical calculation of the vehicle frame with the use of FEM;
- analysis of results from vehicle frame calculations.

Vosco S106 – Polish passenger car developed by the "Syrena" Car Factory in Kutno. In 2012, work on the design of a passenger car began. A stylistic competition entitled "Reactivation of the Polish automotive industry" was announced.

Until 2016 the organizational stage, recruitment of key employees and appointment of Fabryka Samochodów Osobowych SYRENA in Kutno S.A. as an entity to prepare design, prototyping, development and subsequent production of cars, continued.

At the end of 2016, works on the Vosco S106 passenger car were started (Figure 1). The first prototype of Vosco was made in 2017. In April 2018 the vehicle was under homologation tests, in September it received the M1 type approval, it is now ready for production and the first series of this car has already been built. Vosco is to be produced in the quantity of (100-300) pieces a year, in the future production of 1000 pieces is planned.



Fig. 1. Passenger car Vosco S106

In 2017, FSO SYRENA began work on the electric version of the Vosco S106. The project is co-financed by the EU. The Vosco EV car (Figure 2) is based on the same frame construction as the Vosco S106. The components have changed, whose use resulted from the use of a new drive, a set of batteries and the upper part of the structure resulting from R&D works in the project. In the final version of the car, a thorough change of vehicle design is also planned.



Fig. 2. A passenger car with EV electric drive

## 2. Discretization of the 3D geometry of the vehicle frame

On the basis of the 3D model created at the design stage, using the preprocessor in the form of Altair HyperMesh software, the geometry and mesh of the components of the analysed assembly were developed. In the process of discretization of the model (Figure 3), a surface model was created with the use of quadrilateral and triangular elements (Figure 4). In the first stage, a surface model based on the middle surfaces (midsurface) was created from the solid model. Then these surfaces were joined together. It was necessary to ensure the continuity of the grid. A surface mesh with the assumed size of elements was created on the created surfaces [2, 30]. The dominant element size is 5 mm, however, locally this size has been modified in order to accurately reproduce geometry and ensure results closer to reality. The surface elements were given material and geometric characteristics corresponding to those used in the actual structure. The thickness coincident with the thickness of the profile walls, from which the frame elements have been welded, has been defined. The material was defined by giving it the value of the Young's modulus, Poisson's coefficient and the density corresponding to the one used in the construction, i.e. steel. Contacts have been defined in order to map relations between the components of the frame [31, 35, 42].

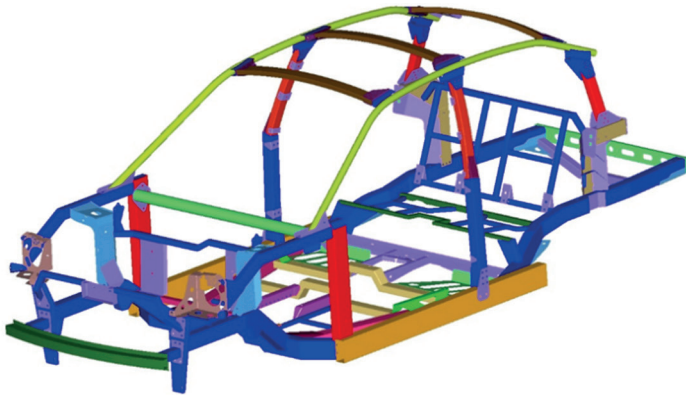


Fig. 3. A discreet model of the vehicle frame grid - isometric projection

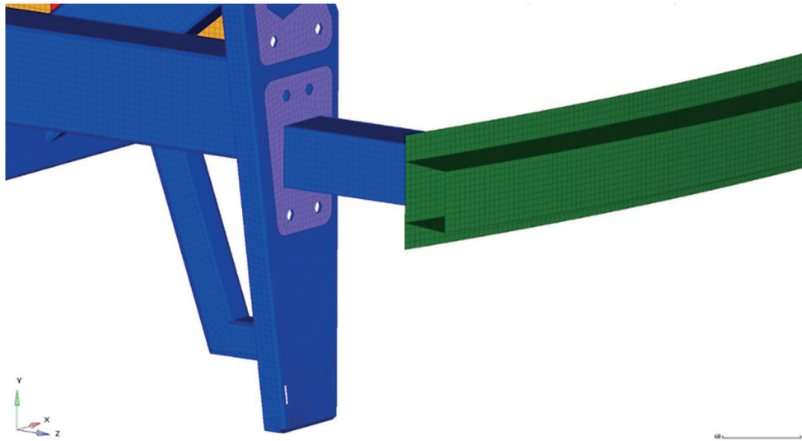


Fig. 4. Examples of discretised components using elements of the quadrilateral and triangular types

The developed discrete connection model was used in the right places of the vehicle frame. In the stage of discretization of vehicle frame geometry, after the analysis of documentation and 3D model, technical simplifications were assumed, in the form of simplifying the shape and the use of RBE elements in the place of standard elements such as screws and welds (Figures 5-6) [36, 37].

The method and place of weld/thread connections prepared in the Altair HyperMesh preprocessor was developed on the basis of the technical documentation received from the client.

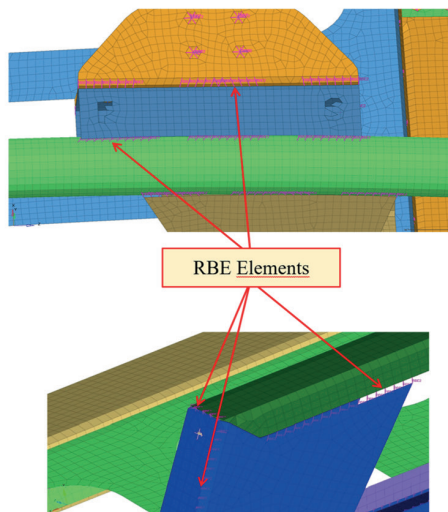


Fig. 5. RBE elements of the OptiStruct numerical solver used in the vehicle frame

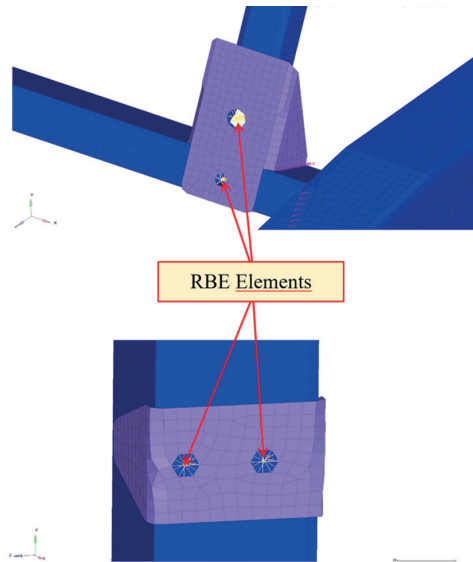


Fig. 6. RBE elements of the OptiStruct numerical solver used in the vehicle frame

### 3. Methodology of Measurements

The measurement was carried out on the beam of the intermediate frame in three places, marked with the following abbreviations: FL – Front Left, FO – Front Center, FR – Front Right, RL – Rear Left, RO – Rear Center, RR – Rear Right. (Figure 7). Due to the digitized nature of the test model, the measurement of deflection must be made on a fixed measuring section. The center of the section will be at the designated points that correspond to the places on the actual intermediate frame. The length of the measuring section is 160 mm, the same as the length of the optical base of the OPK angular level (Figure 19).

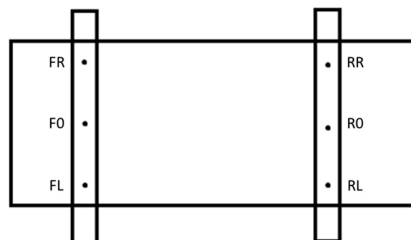


Fig. 7. Scheme of measurement points, where FL – Front Left, FO – Front Center, FR – Front Right, RL – Rear Left, RO – Rear Center, RR – Rear Right

A sub-frame was made to carry out a physical test of torsional stiffness (Figures 8-9).

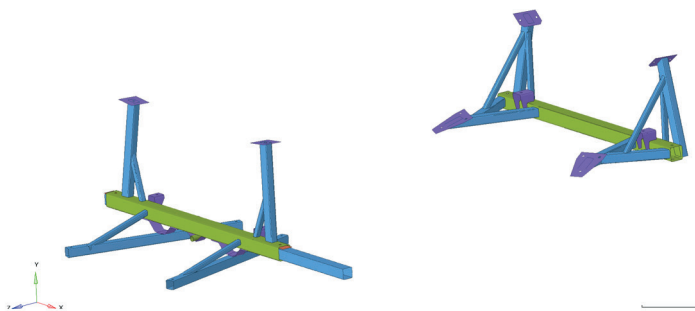


Fig. 8. Intermediate frame

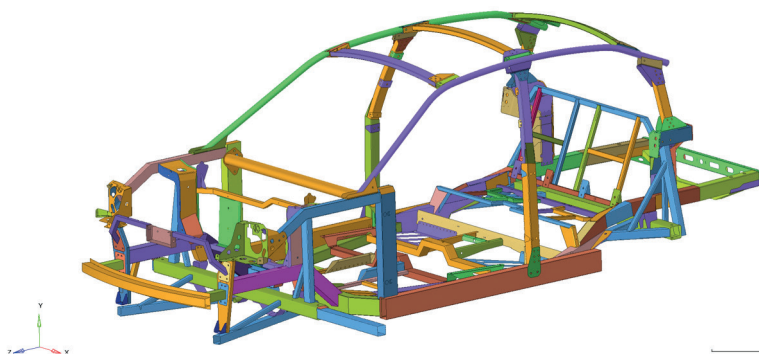


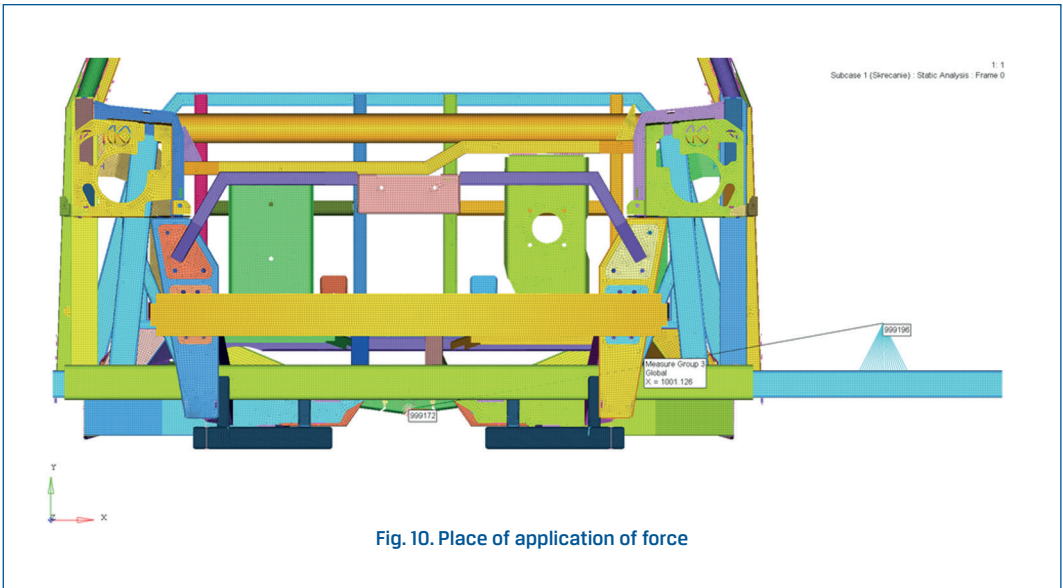
Fig. 9. Intermediate frame attached to the vehicle frame

#### 4. Boundary conditions and defining the load

The discrete model developed for the frame geometry of the vehicle frame, was loaded and fixed in a manner convergent with the method of fixing during the endurance test the actual tested unit.

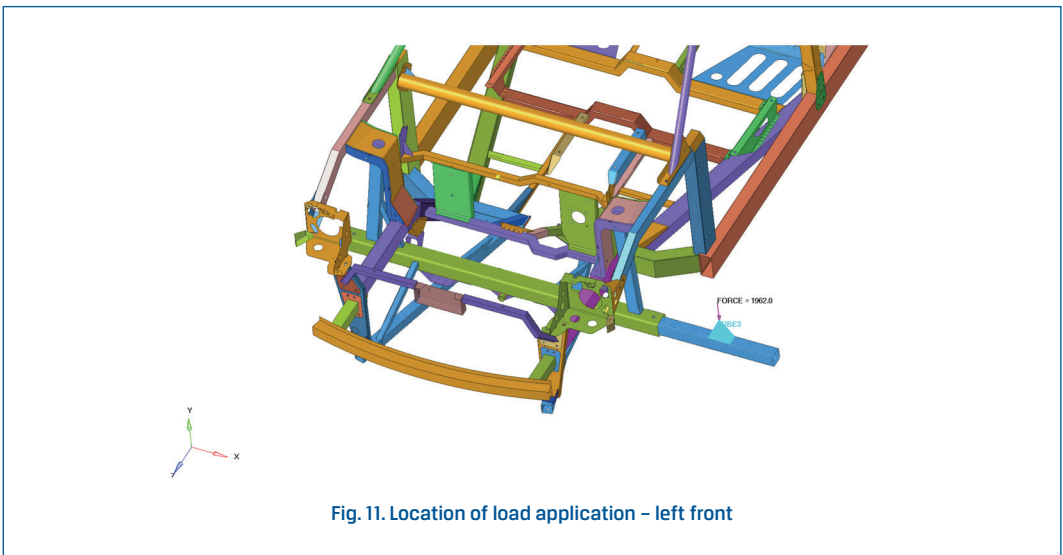
The test load value for the vehicle frame as agreed with the customer was 1962 N (200 kg) and 2550.6 N (260 kg). The load was applied to the intermediate frame. The load in the developed discrete model was distributed to the surface via RBE elements (Figures 10-12). The distance of the applied force to the center of rotation is 1 m.





The load was applied to the beam at a distance of 1000 mm from the axis of rotation.

The distribution of force took place through RBE3 elements in the area covering the width of the beam and the length of 100 mm. The fixing points for the front and rear rotation are shown in the figures (Figures 13-15). Load value: 1962 N (200 kg) and 2550.6 N (260 kg). These loads corresponded to the weight of the weights used during the test on the actual object. In all analysis configurations, both the method of attachment and the application and distribution of force have been defined in the same way.





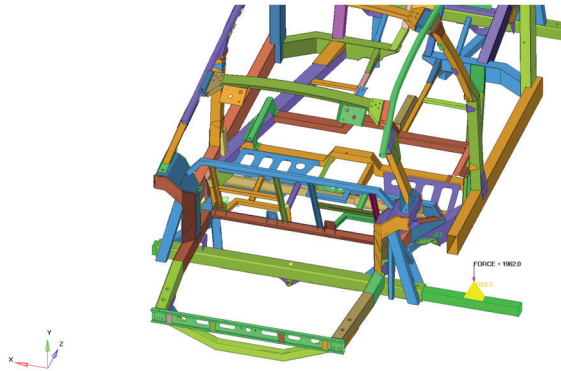


Fig. 12. Location of load application – right rear

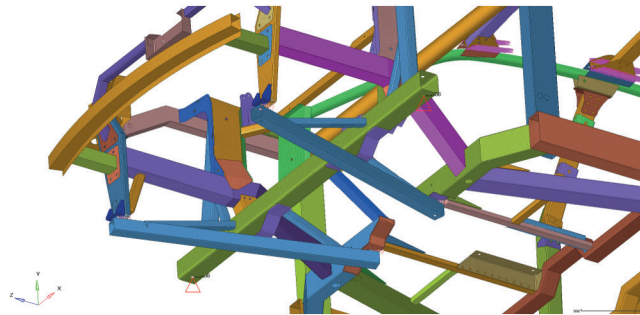


Fig. 13. Mounting location – front

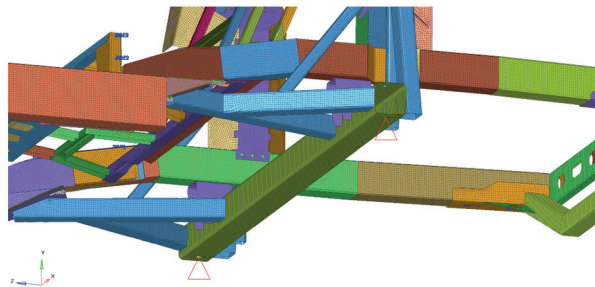


Fig. 14. Location of mounting of the frame – rear

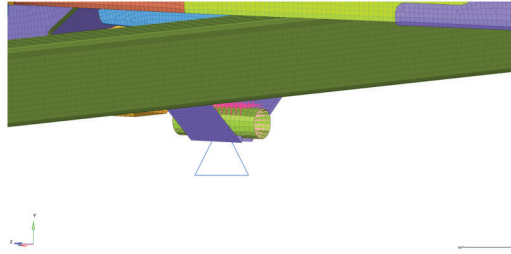


Fig. 15. Placement of the rotation axis - possibility of rotation around the "Z" axis and displacement along the "Z" axis

## 5. List of results of numerical analyses and calculation of stiffness

The following are examples of results of numerical analysis. The figures below show reduced displacements (Figure 16) and displacements in the vertical axis (Figure 17) [18, 22].

Load applied from the right side - rear (RR) – 260 kg

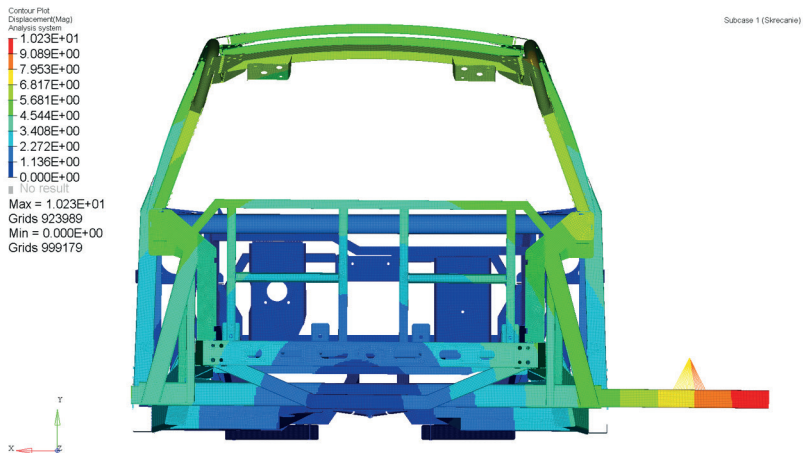


Fig. 16. Reduced displacement (RR) – 260 kg

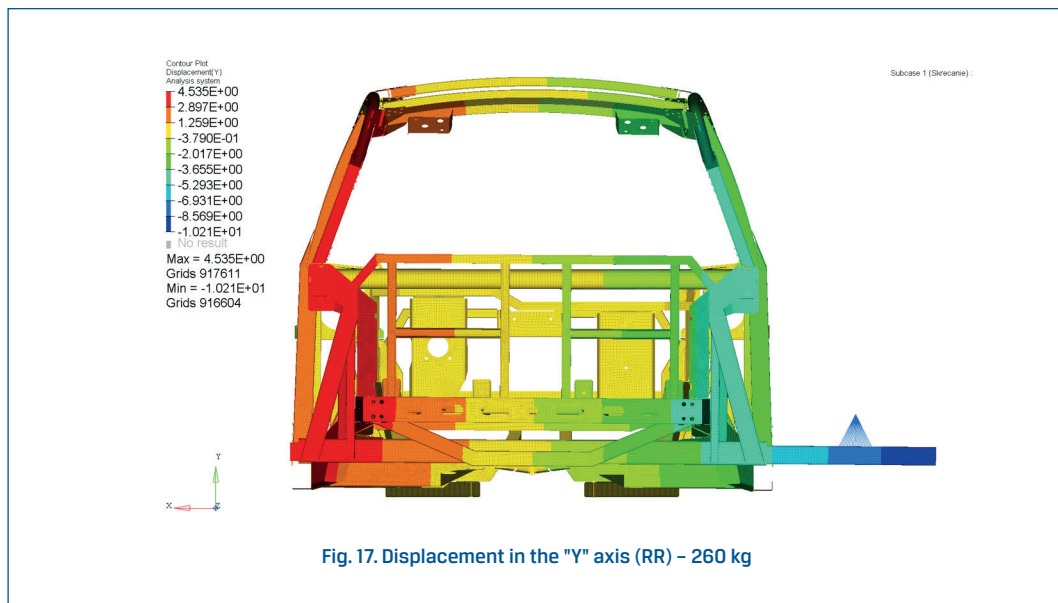


Fig. 17. Displacement in the "Y" axis (RR) – 260 kg

The torsional stiffness of the body  $k_{\phi}$  is the ratio of the change in the torque of the body to change the angle of its sprain, according to the formula:

$$k_{\phi} = \Delta M / \Delta \phi \quad (1)$$

Knowing the geometrical quantities (force arm) and the value of the applied load, we can estimate the moment and by measuring the angle change, we are able to calculate the torsional rigidity of the frame or vehicle body (Table 1). It should be emphasized that depending on the section on which the body is bolted, we will get different values of its torsional stiffness [14, 25].

When developing the results, the place of restraint of the body and the place where the load is applied must be provided [15, 24, 26].

Tab. 1. Summary of results from the conducted analyses, measurement on the beam

Mark	Front			Rear			Stiffness [Nm/°]
	FL [°]	FO [°]	FR [°]	RL [°]	RO [°]	RR [°]	
B1.1.200	0	0	0	0.266	0.288	0.317	<b>6813</b>
B1.1.260	0	0	0	0.345	0.374	0.413	<b>6820</b>
B1.2.200	0	0	0	0.319	0.289	0.268	<b>6789</b>
B1.2.260	0	0	0	0.415	0.376	0.348	<b>6784</b>
B1.3.200	0.265	0.288	0.312	0	0	0	<b>6813</b>
B1.3.260	0.345	0.377	0.410	0	0	0	<b>6766</b>
B1.4.200	0.315	0.290	0.265	0	0	0	<b>6766</b>
B1.4.260	0.406	0.374	0.343	0	0	0	<b>6820</b>

## 6. Study of the real frame

### Boundary conditions

The location and method of fixing the frame of the tested vehicle to the intermediate frame, which is attached to the test stand and to which the assumed load is applied, is presented below (Figure 18) [6, 9, 17].

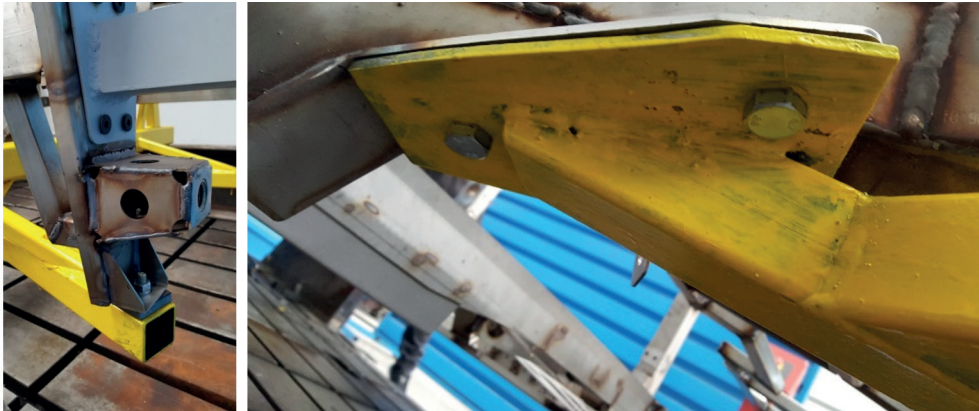


Fig. 18. Location of intermediate frame fixing with front fastening of the sledge and the rear beam

### Measurement method

The torsion angle was measured using the optical angle level OPK. The protractor allows measurement with accuracy of one minute. Angle measurement consisted in setting the protractor on the beam in one of three fixed measuring points. In order to obtain the result, one had to use the knob /3/ to set an air bubble on the level between two straight lines /2/, which meant that the protractor was horizontal. Next, the protractor was directed to the light source and the angle value from the scale was read looking through the viewfinder /1/.

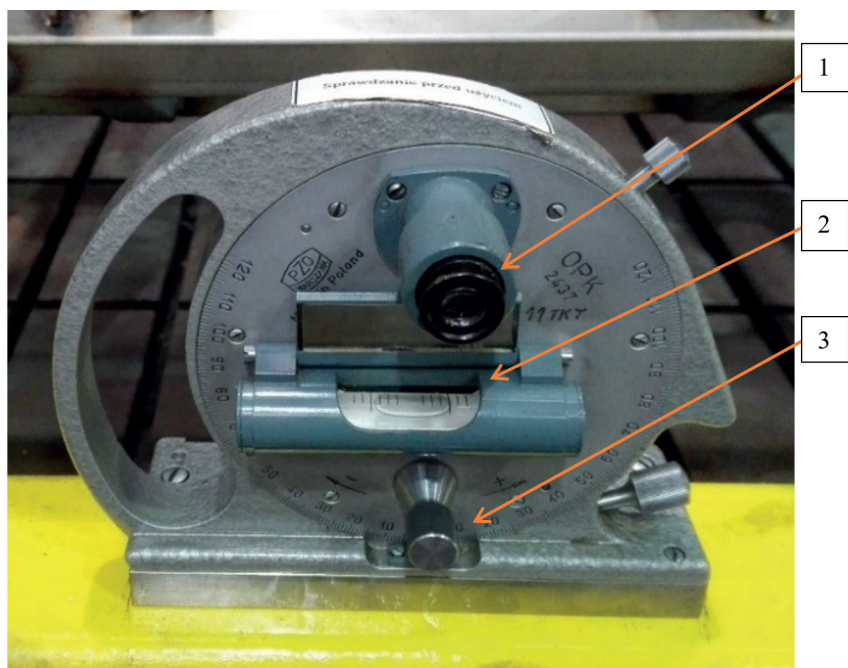


Fig. 19. Application of a protractor

Before starting the measurement, the torsional values without load were read for each variant (B1, B2, B3, B4) (Table 2). In this way, the zero values of the frame twisting were determined. Then the frame was loaded on the shoulder 1 m, with weight of 200 kg. The deflection angles were read at all test points. The weight was increased to 260 kg, the deflection angle values were read again. The last reading was done again at a weight of 200 kg [11, 12, 20].

Tab. 2. Markings used in the conducted tests

A detailed description of the designation in the test	
Bx.1 - FF. RM. R.	Front Fixed-Rear Movable-Right side loaded
Bx.2 - FF. RM. L.	Front Fixed-Rear Movable-Left side loaded
Bx.3 - FM. RF. P.	Front Movable - Rear Fixed - Right side loaded
Bx.4 - FM. RF. L.	Front Movable -Rear Fixed - Left side loaded
B1.1.0	First test with a load of <b>0 kg</b>
B1.1.200.1	First test with a load of <b>200 kg</b>
B1.1.260	First test with a load of <b>260 kg</b>
B1.1.200.2	Test first again with a load of <b>200 kg</b>

## Twisting the front part of the frame

The place and manner of applying the load to the frame of the tested vehicle by means of an intermediate frame, which is attached to the test stand, is presented below. The load is made using a set of weights (Figure 20) [19, 21].

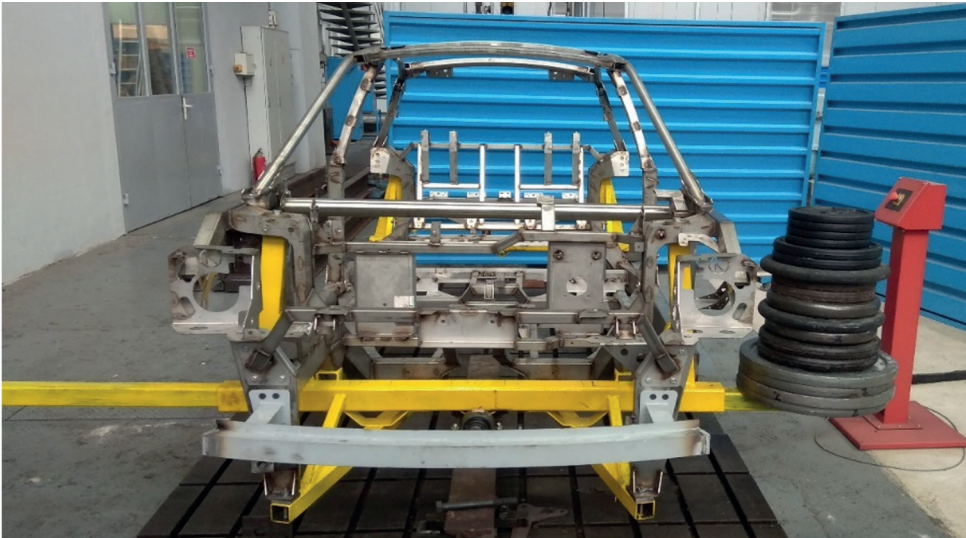


Fig. 20. Example load method – 260 kg, load from the left side – front (FL)

Input data:

Distance from the pivot point:

- $L = 1000 \text{ mm}$

Load:

- $1962.0 \text{ N}$  (200 kg)
- $2550.6 \text{ N}$  (260 kg)

Moment:

- $1962.0 \text{ Nm}$
- $2550.6 \text{ Nm}$

The value of the gravitational acceleration:

- $g = 9.81 \text{ m/s}^2$

Stiffness:

- $k_{\phi} = \Delta M / \Delta \phi \text{ [Nm/}^{\circ}\text{]}$



## 7. List of results obtained from the test on the real object

The table below presents a summary of the results from the tests carried out on the real object. These results were compared with the results of numerical analyses and used in the validation of models and the assumed methodology (Table 3).

Tab. 3. List of results

Mark	Front			Rear			Stiffness [Nm/°]
	FL [°]	FO [°]	FR [°]	RL [°]	RO [°]	RR [°]	
B1.1.0	0.233	0.067	-0.133	0.067	-0.083	-0.233	
B1.1.200.1	0.233	0.067	-0.117	-0.233	-0.367	-0.550	<b>6925</b>
B1.1.260	0.233	0.067	-0.133	-0.300	-0.450	-0.650	<b>6956</b>
B1.1.200.2	0.233	0.067	-0.133	-0.233	-0.367	-0.550	<b>6925</b>
B1.2.0	0.233	0.067	-0.133	0.033	-0.100	-0.267	
B1.2.200.1	0.233	0.067	-0.133	0.317	0.200	0.017	<b>6540</b>
B1.2.260	0.233	0.067	-0.133	0.417	0.283	0.100	<b>6654</b>
B1.2.200.2	0.233	0.067	-0.133	0.317	0.200	0.017	<b>6540</b>
B1.3.0	-0.283	-0.100	0.133	-0.033	0.067	0.217	
B1.3.200.1	-0.017	0.200	0.417	-0.017	0.067	0.217	<b>6540</b>
B1.3.260	0.083	0.267	0.500	-0.033	0.067	0.217	<b>6956</b>
B1.3.200.2	0.000	0.200	0.417	-0.033	0.067	0.217	<b>6540</b>
B1.4.0	-0.267	-0.083	0.133	-0.050	0.083	0.200	
B1.4.200.1	-0.583	-0.367	-0.133	-0.050	0.083	0.217	<b>6925</b>
B1.4.260	-0.667	-0.450	-0.217	-0.050	0.083	0.217	<b>6956</b>
B1.4.200.2	-0.583	-0.367	-0.133	-0.050	0.083	0.217	<b>6925</b>

## 8. Summary of results and conclusions

The assumptions adopted for modelling the vehicle enabled the development of its computational model with the maximum possible mapping of reality, enabling the calculation of strength of the frame with the adopted extortions.

The obtained results of strength calculations, in addition to estimating the torsional stiffness of the vehicle frame, also indicate areas of the structure for which special attention should be paid during operational tests. An additional goal of the numerical analysis was to capture critical points in the structure (places of stress accumulation) [10, 13, 16].

Distortion results, and thus torsional rigidity, obtained from the OptiStruct solver and real tests are convergent with each other. The analyses were carried out for the frame itself.

Tests of the frame torsional stiffness together with the door, the plating, suspension components, engine, transmission and other components increasing stiffness, would give a much better result, because such a construction would constitute a reinforced half-shell.



Another important aspect is the adequate balance of the rigidity of the structure and the assumed vulnerability of the frame elements, essential in the analysis of passive safety during the impact. Properly designed crumple zone must assume a significant deformation of appropriate body fragments, so that the collision energy is properly decelerated and delays occurring during the collision are on the appropriate level, defined in the Regulations UNECE 94 and 95, and thus provide a chance of survival for the driver and passengers. The construction, however, cannot be too limp, so that the inside of the cabin will not penetrate and passengers will not be injured. It is also important to meet the requirements of UNECE Regulation No. 12, which says that the displacement of steering system components must not exceed the assumed values.

Too high stiffness of the body may deteriorate the directional stability of the car movement. Because there are uncontrolled displacements of the attachment points of suspension and steering elements, caused by dynamic forces, e.g. from road unevenness, there may be a change in the angles of the wheel alignment, making the vehicle's steering characteristics deviate from the nominal one assumed in the design process (active safety) [33, 39].

In the construction of the Vosco S106, all these important design aspects have been considered (Table 4) [34, 40, 43].

**Tab. 4. Example values of torsional stiffness of passenger car bodies [23]**

<b>Car model</b>	<b>Torsional Stiffness [Nm/°]</b>
Vosco S106	6956
Opel Astra I	8000
Opel Astra II	12000
Opel Astra II coupe	18000
Opel Astra III	14500
VW Golf II	8620
VW Golf III	11100
VW Golf IV	16500
Ford Focus I	14400
Fiat Punto II 3d	12750
Fiat Punto II 5d	15000
Alfa Romeo 147 3d	19200
Alfa Romeo 147 5d	16500
Peugeot 607	18500
Peugeot 307 SW	18500
Saab 9_3 Sport Sedan	22000
Saab 9_3 Cabriolet	11500
BMW series 5	25000
BMW series 7	27000
Jaguar K-Type wagon	16300

The table below shows a comparative summary of the results of the tests conducted on the real object and the results from numerical analyses (Tables 5-6).

**Tab. 5. Summary of results for a load of 200 kg**

	Real [Nm/°]	Simulation [Nm/°]	Difference [%]
RR (Rear Right)	6925	6813	1.64
RL (Rear Left)	6540	6789	3.67
FR (Front Right)	6540	6813	4.00
FL (Front Left)	6925	6766	2.34

**Tab. 6 List of results for a load of 260 kg**

	Real [Nm/°]	Simulation [Nm/°]	Difference [%]
RR (Rear Right)	6956	6820	1.99
RL (Rear Left)	6654	6784	1.91
FR (Front Right)	6956	6766	2.81
FL (Front Left)	6956	6820	1.99

The above data show the rigidity of vehicles with a welded semi-shell structure. Direct comparison of vehicles with a frame-based design would be sensible after covering the plating and other components of the structure, constituting elements and knots that increase the stiffness of the vehicle. The covering of the above parts in the finished body significantly increases the stiffness of the structure. The following results show that the prepared numerical model, the type of numeric solver used, the assumed simplifications, material models, the manner in which the load was implemented and other aspects of the simulations carried out were well chosen. The correlation between the test results on the real object and the results of the carried out numerical analyses is sufficiently high (within 4%). Assumptions, material models and applied analysis settings led to the correct validation of the numerical model.

Experience and knowledge resulting from the above trials and analyses will be used in the future while creating similar experiments and trials. They will also form the basis for further work on the optimization of the construction, models and vehicle design process.

## References

- [1] Anand A.: Torsional analysis of the chassis and its validation through Finite Element Analysis, India Altair Technology Conference. 2017.
- [2] Barszcz Z., Podkowski K., Seńko J.: Analizy numeryczne MES ramy samochodu Syrenka S201. *Autobusy : technika, eksploatacja, systemy transportowe*. 2016, 6, 782-784.
- [3] Boeman R.G., Johnson N. L.: Development of a Cost Competitive, Composite Intensive, Body-in-White. *Development*. 2002, 1, 1905-1912, DOI: 10.4271/2002-01-1905.
- [4] Borkowski W., Konopka S., Prochowski L.: *Dynamika maszyn*. WNT. Warszawa 1996.
- [5] Braess H.H., Seiffert U.: *Handbook of Automotive Engineering*, SAE, United States of America, 2005.
- [6] Bretl J., Conti P.: Rigid Body Mass Properties from Test data, *Proceedings of the 5th IMAC*. 1987, 655-659.

- [7] Brown, J.C., Robertson, A.J. Serpento, S.T. : Motor Vehicle Structures: Concepts and Fundamentals. Butterworth-Heinemann, Oxford, 2002.
- [8] Cannon R.H.: Dynamika układów fizycznych. WNT. Warszawa 1973.
- [9] Catbas F.N., Lenett M., Brown D.L.: Modal analysis of multiple reference impact test data for steel stringer bridges. Proceedings of the 15th IMAC 1997.
- [10] Catbas F.N., Lenett M., Atkan M., Brown A.E.: Damage detection and condition assessment of Seymour bridge. Proceedings of the 16th IMAC 1998, p. 1694-1702.
- [11] Claisse A., Featherston C.A., Holford K.M., Holt C.A., Manning D.: Measuring the Torsional Stiffness of a Space Frame Chassis using 3D Motion Capture Techniques, Applied Mechanics, and Materials, 2006, 423-428, DOI: 10.4028/www.scientific.net/AMM.3-4.423.
- [12] Crocombe A., Sampe E., Somiotti A.: Chassis Torsional Stiffness: Analysis of the Influence on Vehicle Dynamics. SAE 2010 World Congress & Exhibition, 2010, DOI: 10.4271/2010-01-0094.
- [13] Cuppens K., Sas P., Hermans L.: Evaluation of the FRF based substructuring and modal synthesis technique applied to vehicle FE data, Seminar on Modal Analysis 2001, Department of mechanical engineering division PMA KU Leuven Belgium.
- [14] Deleener J., Mas P., Cremers L., Poland J.: Extraction of static car body stiffness from dynamic measurements. SAE Paper 2010-01-0228 2010, DOI: 10.4271/2010-01-0228.
- [15] Demeester F., Van Brussel H.: Experimental compliance breakdown and real-time optical deformation measurement of flexible manipulators, PhD Dissertation KULeuven Departement Werktuigkunde Celestijnlaan 300B 3001 Heverlee (Belgium), 1992.
- [16] Fregolent A., Sestieri A.: Identification of rigid body inertia properties from experimental data. Mechanical systems and signal processing. 1996, 10, 697-709, DOI: 10.1006/mssp.1996.0047.
- [17] Griffiths D., Aubert A., Green E.R. Ding J.: A technique of relating vehicle structural modes to stiffness as determined in static determinate tests. SAE Paper. 2003-01-1716, DOI: 10.4271/2003-01-1716.
- [18] Hartog J.P.D.: Advanced Strength of Materials, McGraw-Hill Book Co, New York, NY, 2014.
- [19] Helsen J., Cremers L., Mas P., Sas P.: Global static and dynamic car body stiffness based on a single experimental modal analysis test. Proceedings of ISMA2010 Including USD2010.
- [20] Hermans L., Mas P., Leurs W., Boucart N.: Estimation and use of residual modes in modal coupling calculations: a case study. Proceedings of the 18th IMAC. 2000, 930-936.
- [21] Heylen W., Lammens S., Sas P.: Modal Analysis Theory and Testing, Katholieke Universiteit Leuven, Departement Werktuigkunde, Leuven 1997.
- [22] Hibbeler, R.C.: Mechanics of Materials, Pearson Prentice Hall, Upper Saddle River, U.S.A, 2008.
- [23] Instytut Pojazdów PW, Badanie sztywności skrętnej nadwozia (instrukcja do ćwiczenia).
- [24] Lampert J.K., Law E.H., Thompson L.L.: Design of a Twist Fixture to Measure the Torsional Stiffness of a Winston Cup Chassis. Motorsports Engineering Conference and Exposition. 2000, DOI: 10.4271/983054.
- [25] Law E.H., Raju S., Thompson L.L.: Design of a Winston Cup Chassis for Torsional Stiffness. Motorsports Engineering Conference and Exposition. 1999, DOI: 10.4271/983053.
- [26] Law E.H., Raju S., Soni P.H., Thompson L.L.: The Effects of Chassis Flexibility on Roll Stiffness of a Winston Cup Race Car. Motorsports Engineering Conference Proceedings. 1998.
- [27] Gokhale N. S., Thite A.N.: Practical Finite Element Analysis, Altair 2015.
- [28] Pawłowski J.: Nadwozia samochodowe. WKiŁ Warszawa 1964.
- [29] Pawłowski J.: Nadwozia samochodowe. Funkcja użytkowa i struktura nośna. WKiŁ, Warszawa 1978.
- [30] Barszcz Z., Podkowski K., Seńko J.: FEM (Finite Element Method) Numeric Analyses of the Syrenka S201 Car Model. Proceedings of the 13th International Scientific Conference: Computer Aided Engineering, Lecture Notes in Mechanical Engineering, DOI 10.1007/978-3-319-50938-9\_43.
- [31] Rediers B., Yang B., Juneja V.: Static and dynamic stiffness-One test both results, Proceedings of the 16th IMAC 1998.

- [32] Reichelt M.: Identification schwach gedämpfter systeme am beispiel von Pkwkarosserien Doktorarbeit BMW AG 2003-Fakultät für Maschinenbau der Technischen Universität Chemnitz.
- [33] Reński A.: Zastosowanie pomiaru sztywności skrętnej nadwozia do oceny jego jakości. Zeszyty Naukowe Instytutu Pojazdów. Politechnika Warszawska 2002, 4(47), 35-42.
- [34] George A.R., Riley W.B.: Design, Analysis and Testing of a Formula SAE Car Chassis. SAE Motorsports Engineering Conference and Exhibition. 2002, DOI: 10.4271/2002-01-3300.
- [35] Rusiński E.: Metoda elementów skończonych. WKiŁ, Warszawa 1994.
- [36] Rusiński E., Moczko P., Czmochoowski J.: Numerical and experimental analysis of a mine's loader boom crack. Automation In Construction. 2006, 17, 271-277. DOI: 10.1016/j.autcon.2007.05.010.
- [37] Rusiński E., Kopczyński A., Czmochoowski J.: Tests of thin-walled beams joined by spot welding. Journal of Materials Processing Technology. 2004, 157/158, 405-409, DOI: 10.1016/j.jmatprotec.2004.09.063.
- [38] Seidel T.: Rozwój konstrukcji nadwozi.
- [39] Tebby S., Esmailzadeh E., Barari A.: Methods to Determine Torsion Stiffness in an Automotive Chassis. Computer-Aided Design & Applications. 2011, 67-75, DOI: 10.3722/cadaps.2011.PACE.67-75.
- [40] Thompson L. L., Lampert J. K., Law E. H.: Design of a Twist Fixture to Measure the Torsional Stiffness of a Winston Cup Chassis. SAE Paper 983054.
- [41] Tuijelaars L., van der Tas R.: Statics from dynamics. Masterthesis Hogeschool van Arnhem en Nijmegen 2009.
- [42] Zienkiewicz O.C., Taylor R.L.: The Finite Element Method. Fourth Edition, McGraw-Hill, Berkshire, England, 1991, 1-2.
- [43] Żółtowski B.: Badania dynamiki maszyn. Markar-BZ. Bydgoszcz 2002.